Research Article

Evolution of the paleo-Daesan Bay (Nakdong River, South Korea) as a result of Holocene sea level change

Jaesoo Lim[a,b*] 🔵 , Sangheon Yi[a,b*], Min Han[a], Sujeong Park[c] and Youngeun Kim[a,d]

[a]Quaternary Environment Research Center, Korea Institute of Geoscience and Mineral Resources, Daejeon, 34132, Republic of Korea; [b]Korea University of Science and Technology (UST), Daejeon, 34113, Republic of Korea; [c]Department of Marine Sciences and Convergent Technology, Hanyang University Ansan, 15588, Republic of Korea and [d]Department of Astronomy, Space Science and Geology, Chungnam National University, Daejeon, 34134, Republic of Korea

Abstract

To explore sea level transgression in low-lying inland areas and its possible influence on prehistoric cultures, we investigated the physical and geochemical features of 20-m-long sedimentary cores from the previously seawater-filled Daesan Basin located in the middle reach of the present Nakdong River in Korea as proxies for seawater transgression deep inland areas due to Holocene sea level rise. Based on the relationships among grain size, total sulfur content (TS%), and carbon/sulfur (C/S) ratio, the first transgressive event was detected at ca. 8500 cal yr BP, caused by seawater influx along the present Nakdong River. Higher TS% (0.8–1%) and interbedded fossil oysters at 8000–6000 cal yr BP indicate marine environments, supporting a paleo-Daesan Bay with water depth of ∼10–8 m. The common peaks in TS%, in both inland paleo-Daesan Bay and a present coastal area (Suncheon Bay) in southern Korea (e.g., at 3200 and 4700 cal yr BP), may indicate intervals of higher salinity, which suggests simultaneous responses to changes in sea level or hydroclimate. The duration of marine environment (paleo-Daesan Bay) in the remote inland from ca. 8000–3200 cal yr BP provides an analog for inland paleo-bay studies in East Asia.

Keywords: Holocene transgression, Nakdong River, Sulfur content, C/S ratios, Prehistoric culture

(Received 30 November 2021; accepted 18 March 2022)

INTRODUCTION

Information about past coastal environmental changes is essential to understanding past sea level changes and ensuring sustainable development of coastal areas in light of predicted global warming, as well as to tracing past human activities in coastal and surrounding areas. In recent decades, many studies have focused on reconstruction of past sea level changes and their influences on geomorphological changes. Some studies have successfully redrawn past coastlines and geomorphological changes based on reconstructed sea level changes (Stanley and Warne, 1994; Nguyen et al., 1998; Kato et al., 2003; Nahm et al., 2008; Yang et al., 2008; Ishihara et al., 2012; Tanigawa et al., 2013; Lambeck et al., 2014, and references therein; Katsuki et al., 2017; Xiong et al., 2020). Regarding Neolithic cultures, Holocene sea level transgression and climate changes were clearly linked to various early Neolithic settlements in East Asia (Zong et al., 2011; Li et al., 2018; Innes et al., 2019; Sun et al., 2019; Huang et al., 2021). However, the specific timing of the highest transgression level in the Early Holocene is controversial. The effects of subsequent sea level rises and falls on the development of Neolithic societies in various areas during the Late Holocene remain unclear.

Compared to present coastal areas, it is much more difficult to trace the influences of past sea level on inland areas significantly affected by Holocene transgression, particularly in remote locations far away from present coastal areas. In Korea, there is prehistorical evidence that human activities and artifacts in remote inland areas from the Early–Middle Holocene might have been influenced by the presence of seawater at that time (e.g., Hwang et al., 2013). For example, an inland prehistoric site at Bibong-ri (Fig. 1), located 70 km from the Nakdong River mouth, is considered to have been affected by Holocene transgression based on remains and relics, including wooden boats, shell middens, and marine diatoms (Hwang et al., 2013, and references therein). Recently, it has been suggested that this Bibong-ri site had been used by people who shared the Neolithic pottery tradition over hundreds of years and their relics reveal the use of diverse seasonal marine and terrestrial resources throughout the year based on the archaeobotanical and zooarchaeoloical studies (Kaneko, 2008; Kwak et al., 2020; Kim et al., 2021). To interpret past human activities and their remains in terms of the influence of marine environments, it is essential to constrain possible sea level changes and their spatial influence using high-resolution dating and the exact timing of seawater influences. However, changes in sea level along this coastal area have scarcely been studied. Therefore, we need to compare the long-term environmental evolution along the Nakdong River and the Bibong-ri archeological site with available data on sea level changes, and investigate possible effects of sea level in the study area during the Holocene in terms of changes in sea level and seawater influences.

Past seawater influences in coastal areas can be traced using information about sulfur. In the early 1980s, researchers

CrossMark
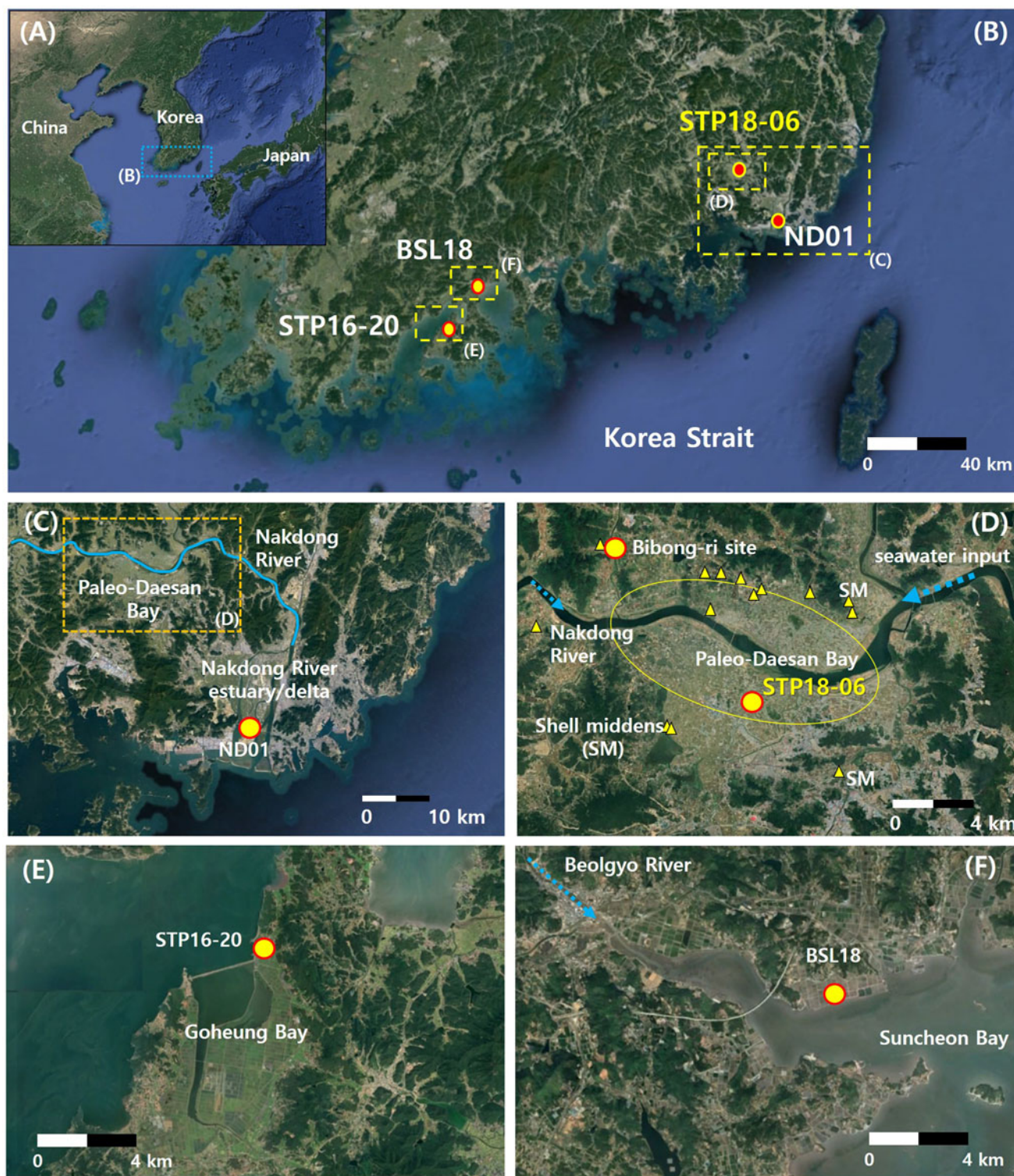
Figure 1. Study area and the collection locations of sedimentary cores discussed in the text. BSL18 (Lim et al., 2015), ND01 (Kim et al., 2015; Cho et al., 2017; Takata et al., 2019), STP16-20 (Lim et al., 2019), and STP18-06 (this study). Yellow triangles in (D) indicate shell middens found around paleo-Daesan Bay.

investigated the environmental context of sulfur (or pyrite) content in coastal sediments. For example, Nakai et al. (1982) tested the meaning of pyrite content, organic carbon isotopes, and the ratio of carbon to nitrogen in the sediments of three embayments of Nagoya harbor in Japan. Their results showed that Holocene climatic and sea level changes controlled these geochemical signals,

with higher pyrite contents during the period of maximum sea level and climatic optimum at a ^{14}C age of 6000–6700 cal yr BP. Similarly, based on the comparison of sulfur content and diatoms in Pleistocene and Holocene sediments from the Shibakawa lowland, northwest of Tokyo in central Japan, Koma and Suzuki (1988) revealed that sulfur content increases with increasing marine

diatom abundance under the influence of seawater invasion into lowland areas. In addition, it has been suggested that, in general, total sulfur is very low in fluvial sediments but has higher levels in marine sediments of ∼0.3–3% (Koma and Suzuki, 1988; Ishihara et al., 2012; Tanigawa et al., 2013; Lim et al., 2015, 2019).

Furthermore, seawater input can change water-quality characteristics, such as salinity. To trace past salinity changes, the carbon/sulfur (C/S) ratio has been used in terms of sedimentary pyrite formation in two end-member environments— marine and freshwater (Berner, 1984; Sampei et al., 1997; Hasegawa et al., 2010; Jaraula et al., 2014). Due to the relatively high availability of dissolved sulfate in seawater, diagenetic pyrite has been suggested to form more readily in marine sediments through a series of geochemical processes driven by sulfate-reducing bacteria compared to freshwater sediments (Berner, 1984; Berner and Raiswell, 1984). In general, marine sediments have C/S ratios of 0.5–5, whereas freshwater sediments have higher C/S ratios (>10), producing two distinct end-members (Berner and Raiswell, 1984). Brackish water shows two ranges depending on the influence of saltwater. Brackish waters with predominantly marine influence have intermediate values (4–11),while those with minor admixtures of marine water have higher ratios of 11–17 (Woolfe et al., 1995, and references therein). Jaraula et al. (2014) reconstructed changes in Holocene salinity in a coastal lake (Lake Laguna de Bay, Philippines) using C/S ratios and suggested that past salinity shifts were linked to sea level changes coupled with tectonic activity and climate change. Discussing the interpretation of TS% and C/S ratios along the coast of Korea, Lim et al. (2015) suggested that during the Early Holocene, TS% and C/S ratios were significantly affected by seawater entering low-lying coastal areas due to transgression. However, during the Middle–Late Holocene, with relatively stable sea level change, the values appear to have been related to salinity changes in coastal areas, which are controlled by changes in freshwater input and linked to hydroclimatic changes.

In addition, freshwater influences in coastal areas can be examined through changes in terrestrial plant input using sedimentary carbon/nitrogen (C/N) ratios. Aquatic plants predominantly have elemental C/N ratios of 4–10, whereas terrestrial plants have relatively high C/N ratios of >12 because they are composed mainly of lignin and cellulose (Meyers, 1997; Lamb et al., 2006, and references therein). Thus C/N ratios from coastal sediments can indicate relative abundance between aquatic plants and land plants, suggesting possible changes in sea level or freshwater input via rivers (e.g, Lamb et al., 2006).

Here, we aim to trace past seawater influences and environmental changes based on TS%, C/S ratio, C/N ratio, and grain size changes in an inland region of the Nakdong River to support the interpretation of archaeological artefacts. This study will deepen the understanding of past sea level-related environmental changes and provide an opportunity to explore the spatial patterns of Holocene transgression along the southern coast of Korea.

STUDY AREA AND METHODS

The study area, Daesan Basin ("paleo-Daesan Bay"), is located in the middle reach of Nakdong River in Korea (Fig. 1). This area is near the prehistorical site at Bibong-ri, located 70 km from the Nakdong River mouth. Based on deposits and artefacts, including wooden boats, shell middens, and marine diatoms, this site is considered to have been affected by Holocene transgression (Hwang et al., 2013). However, few geochemical data are available regarding direct seawater influence, water-depth changes, and the duration of the paleo-bay ("Paleo-Daesan Bay"), all of which are necessary for interpretation of prehistoric cultures.

In the study area (Fig. 1), annual precipitation is ∼1400 mm, and summer rainfall accounts for 70% of total annual rainfall. This area, which has been affected by frequent flooding events driven by heavy summer rainfall, has been reclaimed since the 1970s and used as agricultural fields. To investigate past seawater influences, sedimentary cores of ∼20 m in length were recovered from site STP18–06 (35°19′46.57″N, 128°44′40.53″E, 5.47 m in elevation) and then subsampled at an interval of 10 cm.

To trace the temporal sequence of sediment core STP18–06, we performed ^{14}C dating on plant fragments and shell fragments (oysters) recovered from the core. Pretreatment for ^{14}C dating was done based on previous studies (e.g., Kigoshi et al., 1980; Abbott and Stafford, 1996; Kretschmer et al., 1997). Plant fragments (n = 26) underwent a series of acid-alkali-acid treatments to remove contaminants. Samples of shell fragments (n = 3) were treated with acid to clean the surfaces, then, after washing with distilled water and drying, crushed into powder. After graphitization of the pretreated plant and shell samples, radiocarbon dating was performed using the accelerator mass spectrometry facility of the Korea Institute of Geoscience and Mineral Resources (Hong et al., 2010a, b). ^{14}C ages (conventional radiocarbon dates) were converted to calibrated ages (cal yr BP) using the software OxCal 4.3 (Bronk Ramsey, 2009a, b) and IntCal13 calibration curve (Reimer et al., 2013). Calibrated ages were reported as probability density ranges at the 95.4% confidence level.

For grain-size analyses, ∼300 mg dry samples were treated with 35% H_2O_2 to decompose organic matter and then boiled in 1 N HCl for 1 hour to remove carbonates and iron oxides. After rinsing with distilled water, the samples were treated with an ultrasonicator for 15 seconds to make a suspension and facilitate dispersion. Grain-size analyses were performed using a Mastersizer 2000 laser analyzer (Malvern Instruments, UK).

For total organic carbon (TOC), total nitrogen (TN), and TS analyses, bulk subsamples of core STP18–06 were treated with 1 N HCl at ∼100°C for 1 hour and rinsed with distilled water. Then, each ∼3–5 mg HCl-treated subsample was loaded into a tin combustion cup. Both TOC and TS were determined using a CNS elemental analyzer (Vario Micro Cube; Elementar, Germany), with assumed carbonate-free conditions. Pyrite sulfur and total sulfur are roughly equivalent in most fine-grained sediments (Benner and Raiswell, 1984; Woolfe et al., 1995); therefore, in this study, the C/S ratio and C/N ratio were calculated using TOC/TS and TOC/TN, respectively.

RESULTS

Age dating

Table 1 and Figures 2 and 3 display data from and photos of core STP18–06, which formed during the late Pleistocene and Holocene. The basal part of the core (18.4 m depth) was dated at 44,000 ± 450 ^{14}C yr BP, which suggests a hiatus between Late Pleistocene and Holocene sediments. The uppermost part of the core was deposited during the Late Holocene, as evinced by an age of 2040 ± 30 cal yr BP (5.73 m depth). The age-dating results of shell fragments (oysters, n = 3) found at 13–15 m depth in the core were 6260–7400 cal yr BP, which suggests seawater influence during the Middle Holocene in the study area. Depth (m) was converted into age (cal yr BP) using the age-depth model calculated by CLAM software (Blaauw, 2010) under the following settings: linear interpolation

Table 1. Results of radiocarbon (^{14}C) dating and calibrated dates for core STP18-06.

| Depth (m)	^{14}C yr BP (± 1σ)	cal yr BP (± 2σ)	δ^{13}C (‰)	Lab. code	Dated material
5.73	2037 ± 28	2005 ± 100	−27.97	KGM-IWd200209	Plant fragments
5.97	2019 ± 33	1970 ± 85	−35.51	KGM-IWd200210	Plant fragments
6.57	2253 ± 31	2250 ± 90	−34.05	KGM-IWd200211	Plant fragments
7.3	2900 ± 30	3055 ± 100	−26.99	KGM-ITG170116	Plant fragments
9.64	3280 ± 30	3510 ± 65	−26.26	KGM-ITG170117	Plant fragments
9.81	2178 ± 31	2210 ± 100	−31.57	KGM-IWd200212	Plant fragments
10.5	2977 ± 38	3160 ± 160	−39.23	KGM-IWd200213	Plant fragments
10.53	2964 ± 30	3110 ± 105	−26.99	KGM-IWd200214	Plant fragments
11.01	3050 ± 30	3260 ± 90	−30.44	KGM-ITG170118	Plant fragments
11.04	3092 ± 33	3300 ± 80	−29.45	KGM-IWd200215	Plant fragments
11.31	3239 ± 31	3470 ± 85	−35.97	KGM-IWd200216	Plant fragments
11.4	2980 ± 30	3190 ± 130	−26.87	KGM-ITG170119	Plant fragments
11.7	3040 ± 30	3260 ± 90	−23.19	KGM-IWd200217	Plant fragments
12.11	3650 ± 30	3990 ± 100	−31.34	KGM-ITG170120	Plant fragments
12.8	4679 ± 33	5450 ± 130	−26.36	KGM-IWd200218	Plant fragments
13.05	3924 ± 67	4340 ± 185	−23.61	KGM-IWd200219-1	Plant fragments
13.42	4300 ± 32	4890 ± 65	−21.69	KGM-IWd200220	Plant fragments
13.66	5050 ± 30	5810 ± 90	−29.09	KGM-ITG170121	Plant fragments
13.74	5460 ± 38	6250 ± 60	−2.18	KGM-ICa200054	Shell (oyster)
14.26	6405 ± 41	7340 ± 75	−3.8	KGM-ICa200055	Shell (oyster)
14.42	6473 ± 39	7380 ± 75	−0.89	KGM-ICa200056	Shell (oyster)
16.47	7300 ± 42	8100 ± 80	−32.92	KGM-IWd200221	Plant fragments
16.72	7430 ± 40	8260 ± 80	−29.84	KGM-ITG170122	Plant fragments
16.83	7281 ± 39	8090 ± 80	−28.17	KGM-IWd200222	Plant fragments
17.07	7670 ± 39	8470 ± 70	−29.49	KGM-IWd200223	Plant fragments
17.24	7787 ± 63	8580 ± 165	−41.92	KGM-IWd200224	Plant fragments
17.52	7940 ± 40	8810 ± 170	−33.36	KGM-ITG170123	Plant fragments
18.40	44023 ± 456		−26.55	KGM-IWd200225	Plant fragments

between dated levels (type = 1), weighted by calibrated probabilities (prob = 0.95), dates assumed outlying (outliers, 10 points). Reversed ages (outliers, indicated by red points) were not used.

Lithology and geochemical analyses

As shown in Figure 4, core STP18–06 is comprised of seven lithologic units (Units 1–7). Unit 1 (21–17.45 m) consists of greenish-yellow deposits containing sandy silt in the lower part and oxidized brown mottles in the upper part, slightly fining upward. Unit 2 (17.45–17 m) was characterized by light- to dark-gray deposits of fine silt with gradual fining upward. Unit 3 (17–16.30 m) contained gray sandy silt deposits. Unit 4 (16.30 to 13.60 m) was mainly dark gray silty deposits with plenty of shell (mainly oyster) fragments. An important lithologic feature of Unit 4 is the occurrence of oysters, with two shell layers at 16–15.5 m and 15–13.4 m, showing shell fragments up to 4 cm long. Unit 5 (13.6–7 m) consisted of gray fine-grained sand

deposits and showed a long-term coarsening upward trend with superimposed fluctuations in the percentage of sand between 40–90%. Unit 6 (7–5 m) is fining-upward gray sandy silt. Unit 7 (5–0.8 m) contains gray to yellowish silty deposits. Most of the upper layer was disturbed during reclamation.

As shown in Figure 4, the geochemical stages of core STP18–06 fluctuated significantly. For example, TS% varies from 0–1%, and C/S ratios fluctuate between ~0.2 and 40, which suggests marked environmental changes between marine and freshwater settings. C/N ratios vary between ~12 and 40, with an average of 19.2, which suggests relative abundance changes between terrestrial and aquatic organic matter. Notably, the depth profile of the percentage of sand was very similar to those of TS% and TOC%. This similarity is supported by negative correlations between percentage of sand and TS ($R^2 = 0.56$) and between percentage of sand and TOC% ($R^2 = 0.663$) (Fig. 5). This relationship indicates that fine-grained sediments in the sedimentary cores have high TS% and TOC% values, while coarse-grained sediments
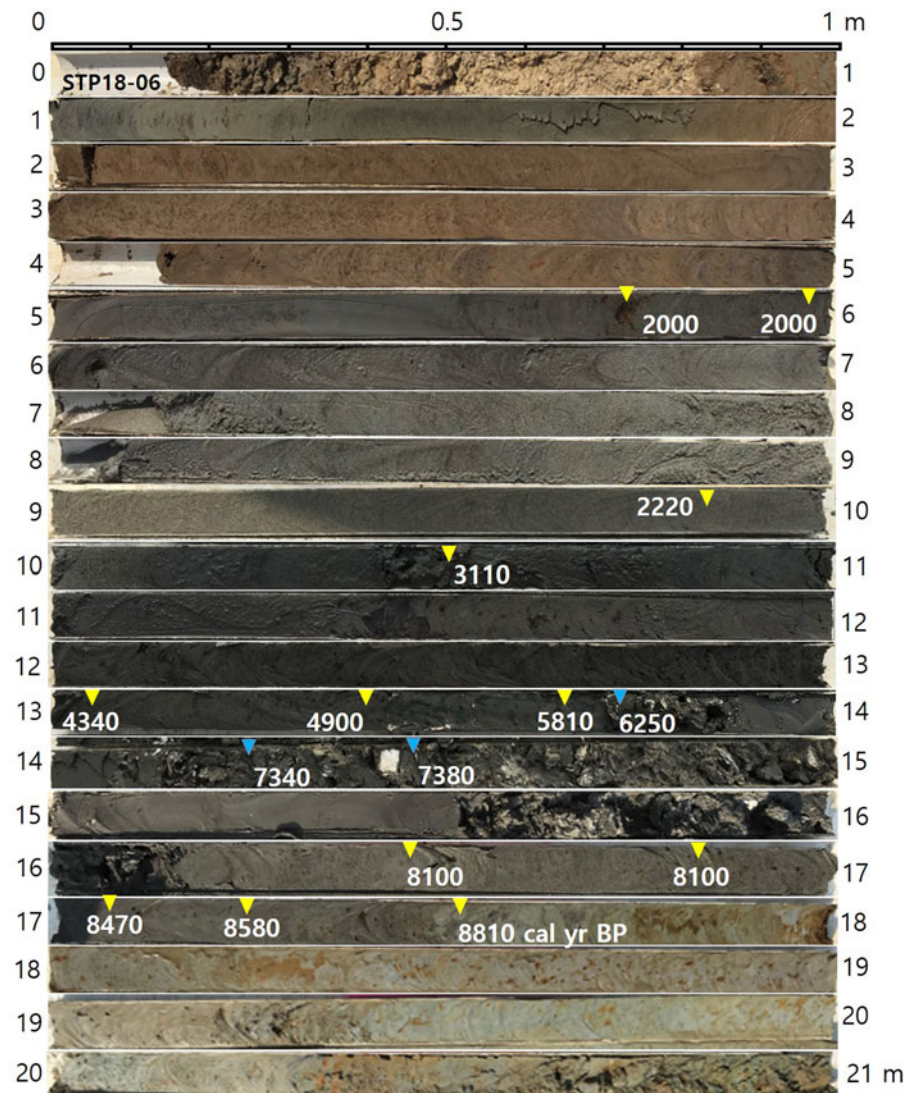
Figure 2. Photograph of sediment core STP18-06 recovered from in the middle reach (called Daesan Plain) of the Nakdong River, Korea. Numbers indicate results of ^{14}C dating of plant fragments (yellow triangles) and shell fragments (blue triangles).

have low values. The sedimentary sequence of core STP18–06 can be divided into nine stages based on the average values of TS%, C/S ratios and C/N ratios (Fig. 4) that represent the Early–Late Holocene.

DISCUSSION

Seawater influence in the paleo-Daesan Plain during the Holocene and links to other coastal environments along the southern coast of Korea

Paleoenvironmental reconstruction in a given area must be compared to those at other sites to test for consistency with local and regional environmental changes. From the regional viewpoint of sea level rise in spatial and temporal terms, changes should have simultaneously influenced coastal areas and inland paleo-bay areas. This process involves shifts from freshwater-dominant to marine-dominant environments due to Holocene sea level rise (Stanley and Warne, 1994; Hori et al., 2004; Kim et al., 2012; Tanigawa et al., 2013; Lambeck et al., 2014, and references therein; Cho et al., 2017; Katsuki et al., 2017; Xiong et al., 2020). To trace specific geomorphological-geochemical settings (e.g., intertidal,

estuary, and inner bay) that formed in response to sea level changes, information about sea level in previous times and paleo-water depth in the study area is essential (e.g., Lim et al., 2015, 2019).

Based on radiocarbon ages, lithostratigraphy, and the results of geochemical analyses, the study area was clearly influenced by seawater transgression, leading to the formation of marine environments during the Early–Late Holocene. The sedimentary sequence of core STP18–06 can be divided into nine stages during the Holocene based on average values of TS% and C/S ratio (Fig. 6). The stages of long-term coastal evolution clearly indicate different environments affected by a combination of sea level and hydrological changes, as explained in the following discussion. We interpret the short-term changes in TS% in terms of regional seawater-influence changes through comparison with TS% changes in Holocene coastal sediments from Goheung Bay (Lim et al., 2019) and Suncheon Bay (Lim et al., 2015).

Stage 1 (before ca. 8700 cal yr BP): freshwater environment
Stage 1 corresponds to lithologic Unit 2, with nearly zero TS% (Figs. 4, 6C). This stage appears to have formed under freshwater conditions with high aquatic organic matter input, as shown in
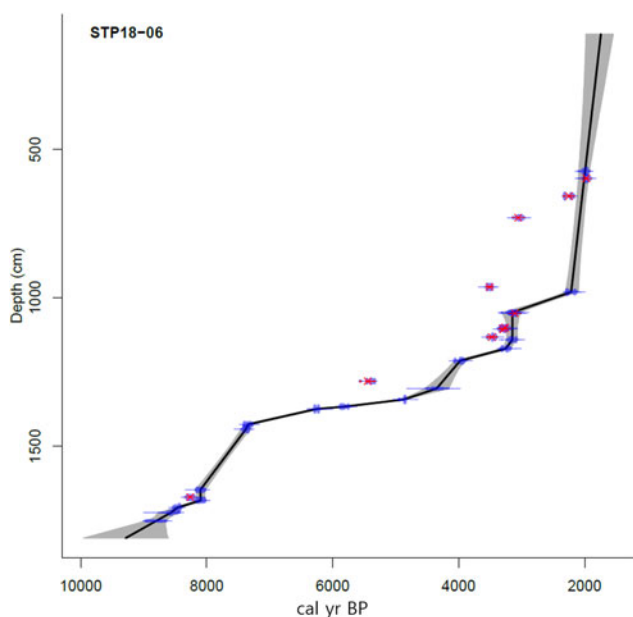
Figure 3. Age-depth model for core STP18–06. Depth (m) was converted into age (cal yr BP) using the age-depth model calculated by CLAM software (Blaauw, 2010). Reversed ages (outliers, indicated by red points) were not used.

decreased C/N ratios (Fig. 4). Interestingly, the depositional elevation of the core STP18–05 site at 8700 cal yr BP was lower by 2–4 m than the STP16–20 site in Goheung Bay (Lim et al., 2019) and BSL18 site in Suncheon Bay (Lim et al., 2015) (Fig. 6A). Along the past Nakdong River channel, prior to ca. 8700 cal yr BP, seawater was located in the present Nakdong River delta area (Yoo et al., 2014). The diatom assemblage of sediment core ND01 (Fig. 1) suggests that the first marine transgression occurred at ca.10.5 ka in the present Nakdong River delta, which evolved into an estuarine environment until 9.8 ka. Since then, due to sea level rise, the Nakdong River mouth region has become an inner bay (Cho et al., 2017), suggesting resultant transgression along the past Nakdong River channel.

Stage 2 (ca. 8700–8300 cal yr BP): first transgression and marine (brackish to estuarine) environment

At this stage, the study area appears to have experienced its first direct seawater influence, as evinced by the increase in TS% from 0–0.8% and decrease in C/S ratio to 1.5 (Fig. 6B, C). Past coastal environmental changes have been traced using TS%, which has different ranges among environments (e.g., ∼0.3% in fluvial sediments and 0.3–3% in marine sediments; Koma and Suzuki, 1988; Ishihara et al., 2012). Regarding salinity changes, marine sediments deposited at high salinity are considered to have low C/S values (0.5–5) compared to freshwater sediments, which have high C/S values (>10) (Berner and Raiswell, 1984). Based on these previous findings, the observed increase in TS% from 0.1% to 0.9% and decrease in C/S ratio to 1.5 suggests an intensified seawater influence, resulting in a ca. 400-year period of marine environmental conditions.

Interestingly, during the period from 8700–8300 cal yr BP, TS % in the core STP18–06 site was higher than in present coastal areas (STP16–20 and BSL18 sites) (Figs. 1, 6E, F). This result suggests that the Deasan area may have been influenced by seawater at that time and may indicate a significant role of the Nakdong channel in rapidly introducing seawater to inland areas in the

past. However, coastal areas, including the sites of STP16–20 (Lim et al., 2019) and BSL18 (Lim et al., 2015), appear to have been disturbed due to higher elevation and the presence of multiple islands, and therefore experienced delayed seawater input.

Stage 3 (ca. 8300–7900 cal yr BP): freshwater environment.

Stage 3 was characterized by a significant return to the conditions of Stage 1, with nearly zero TS% (Fig. 6C). This decrease in TS% was coupled with an increase in grain size, as demonstrated by the increased percentage of sand. This regression and return to a freshwater environment in the paleo-Daesan basin reflect brackish environments with 0.1–0.3% TS at the STP16–20 (Goheung Bay) and BSL18 (Suncheon Bay) sites (Figs. 6E, F). This similarity suggests that the inland area connected by a channel to the open ocean was highly vulnerable to slight changes in sea level or river discharge. Notably, Stage 3 corresponds to an abrupt cooling event, referred to as the 8.2 ka event, which was caused by rapid drainage of proglacial Lake Agassiz-Ojibway and the resulting decrease in the strength of North Atlantic thermohaline circulation (Alley et al., 1997; Törnqvist et al., 2004; Kendall et al., 2008). In coastal areas, decreased TS% has been attributed to the dilution effects caused by increased freshwater input or falling sea level (Lim et al., 2015). Based on pollen analyses, Park et al. (2018) suggested weakened precipitation along the southern coast of Korea during this cold event. Several oxygen isotope-based interpretations of stalagmites in China noted significant decreases in Asian summer monsoon precipitation over China during the 8.2 ka cold event (Dykoski et al., 2005; Hu et al., 2008; Tan et al., 2020). Thus, the decrease in TS% in the study area cannot be explained by decreased precipitation during the cold event. At present, little precipitation information is available for the upper reaches of the Nakdong River, corresponding to mountainous inland areas, during the Early Holocene, including during the 8.2 ka cold event, and therefore further evidence is needed to exclude the possibility of freshwater influence completely.

Stage 4 (ca. 7900–5600 cal yr BP): second transgression and marine (inner bay) environment

This stage is characterized by high TS% values up to 1% and very low C/S ratios varying between 1–3 (Figs. 6B, C), which suggests a second transgression and subsequent marine conditions with high salinity. As described above, the water depth during Stage 4 can be estimated based on the elevations of shell layers at the Bibong-ri site and reconstructions of sea level from Chinese coastal areas and Toyooka Basin, Japan (Fig. 6). The elevations of shell layers in marine sediments from the Bibong-ri site are 7–8 m higher than the depositional surface elevation in core STP18–06 from the paleo-Daesan basin. The reconstructed past sea level curve shows sea level changes between −1 and 1 m during Stage 4. Considered that the depositional surface layers in core STP18–06 are between −11 and −8 m, the estimated water depth during Stage 4, determined from the difference between regional sea level and the depositional surface elevation of the core, appears to have been about 8–11 m. The present tidal range on the south coast of Korea is ∼3 m. If we assume similar tidal ranges in the Early and Middle Holocene, the estimated paleo-water depth of 10 m and marine environment supported by high TS% and low C/S ratios indicate a bay environment during Stage 4, which suggests the existence of paleo-Daesan Bay and supports the previous interpretation of the Neolithic environment in the area (Hwang et al., 2013). Interestingly, the formation of a
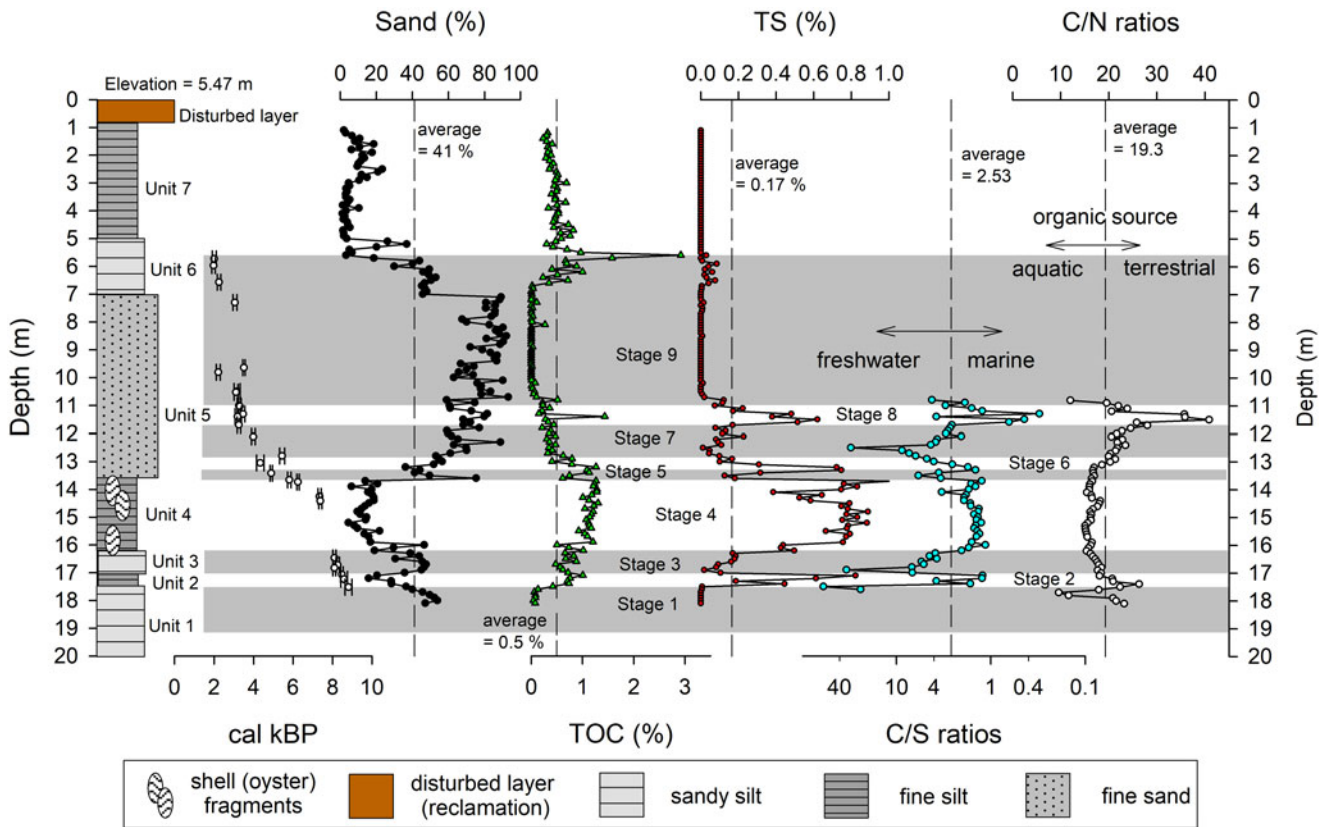
Figure 4. Lithological units, grain sizes (sand%), and geochemical characteristics (TOC%, TS%, C/S ratios, C/N ratios) of core STP18–06, recovered from Daesan Plain in the middle reach of the Nakdong River, Korea. Geochemical features were divided into nine stages based on the average values of TS% and C/S ratio.
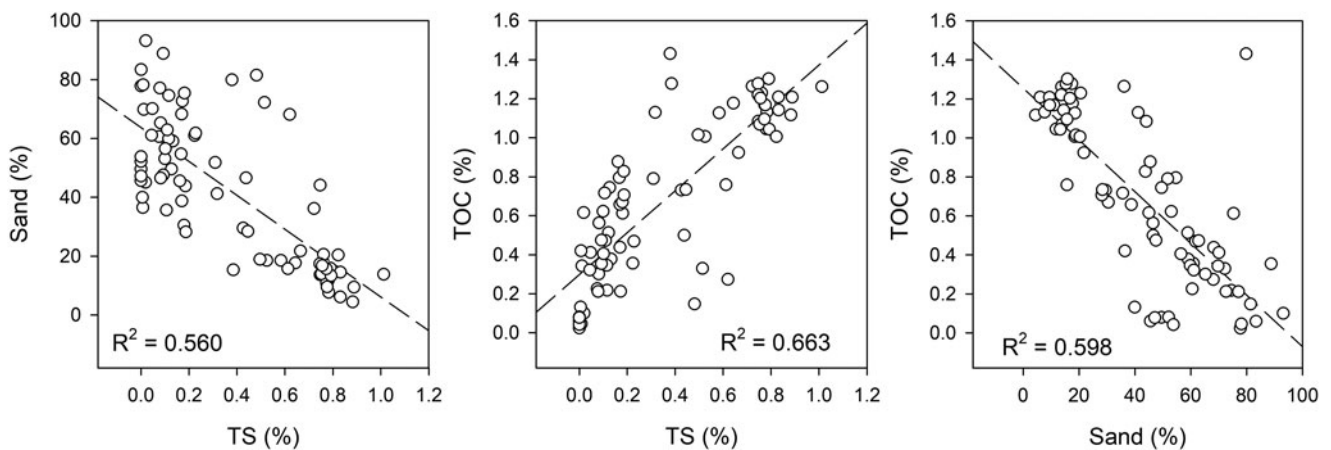
Figure 5. Correlations among sand%, TS%, and TOC% in sedimentary core STP18–06, recovered from Daesan Plain in the middle reach of the Nakdong River, Korea.

bay environment in this stage is similar to the shift after 8 ka from inner to outer bay in the lower reaches of the present Nakdong River, which is supported by increasing numbers of oceanic species in sedimentary core ND01 (Fig. 1) (Cho et al., 2017). The appearance of both benthic foraminifera and warm-water planktonic foraminifera in the inner part of the Nakdong River delta suggests landward movement of benthic foraminifera and intensification of the Tsushima Warm Current in conjunction with sea level rise during the Early–Middle Holocene (Takata et al., 2019).

An important feature of this stage is the occurrence of oysters, with shell layers ~1 m thick. Oysters are observed in fine mud sediments as fragments up to 4 cm long (Fig. 3). The range of radiocarbon dates (6500–7400 cal yr BP) obtained from three oyster fragments suggests oyster growth in the area during at least the Middle Holocene. Regarding possible reservoir effects based on radiocarbon dating of shells from southern coasts during the Holocene, Nakanishi et al. (2013, 2015) suggested that reservoir ages (R) were not constant during the Holocene due to different
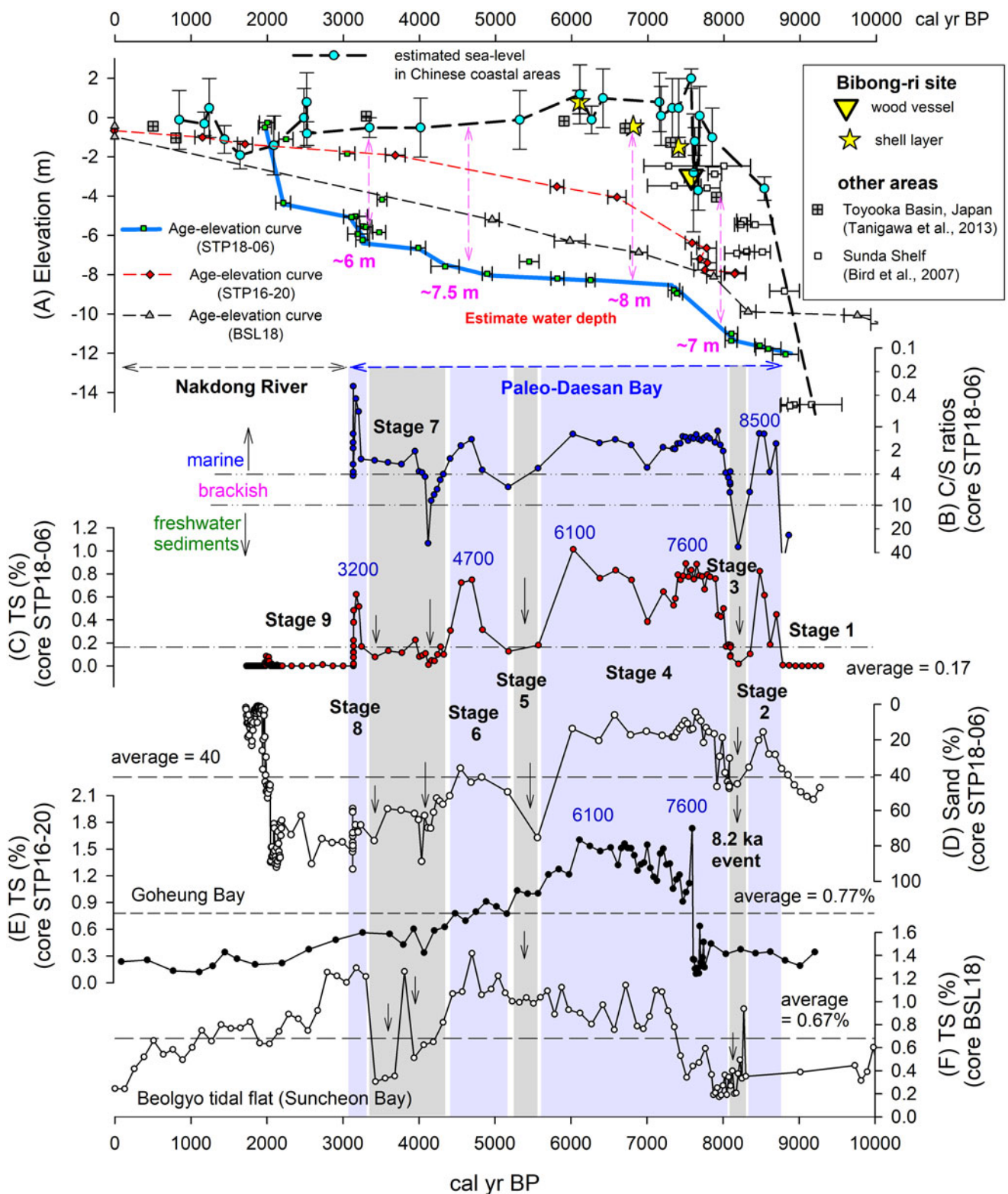
Figure 6. Results indicating depositional environmental changes in core STP18–06, recovered from Daesan Plain in the middle reach of the Nakdong River, Korea, based on comparison with shell middens and a vessel from Bibong-ri site, Korea (Hwang et al., 2013, and references therein), reconstructed sea level changes (Bird et al., 2007; Tanigawa et al., 2013; Lambeck et al., 2014, and references therein), and TS% changes in other coastal areas of Korea (core BSL18 [Lim et al., 2015] and core STP16–20 [Lim et al., 2019]).

extents of seawater input and mixing ratios based on differences between shell and plant data from various coastal sedimentary cores collected along the western and southern coasts of Korea.

They suggested reservoir ages of 430 ± 190 years, within ranges of 60 ± 60 to 1000 ± 60 years, since 9000 cal yr BP. In particular, they showed that average R values in the inner bay sediments have

small ranges (ca. 100 years). Recently, Kim et al. (2021) tested ΔR values in the Pacific database by dating the pre-bomb (pre-1950) blue mussel shell (*Mytilus edulis*) from the southern coastal region of Korea and suggested similar results with ΔR value of −83 ± 16. Thus, each radiocarbon date of three oyster fragments deposited in the bay environment can be considered growth ages within ca. 100 yr of error range.

Stage 5 (ca. 5600–5100 cal yr BP): marine-brackish environment
Stage 5 is a period with significantly decreased TS%, falling to 0.2%, while C/S ratios remained ~4, which suggests a marine-brackish environment (Fig. 6B, C). This decrease in TS% is unclear in Goheung Bay (STP18-20) and Suncheon Bay (BSL18) (Figs. 1, 6E, F), although a slight decrease was observed in Suncheon Bay.

Stage 6 (ca. 5100–4300 cal yr BP): marine environment
This stage represents another strong marine environment with increased TS% up to 0.8% and decreased C/S ratios as low as 1 (Fig. 6B, C). During this stage, the estimated water depth appears to have been ~7 m, which suggests an enclosed bay environment. However, the grain size of sediments decreased, which suggests expansion of the coastal area or weak flooding from the Nakdong River.

Stage 7 (ca. 4300–3200 cal yr BP): brackish environment
The seawater influence in Stage 7 was considerably lower, as demonstrated by decreased TS% (0.1–0.2%), which suggests a brackish environment (Fig. 6C). Interestingly, Stage 7 is characterized by acceleration of coarsening in sediments deposited in the study area. Percentage of sand during this stage increased from 40% to 80% (Fig. 6D). An increase in C/N ratios from 20 to 30 indicates intensified input of terrestrial organic matter via the river (Fig. 4). This shift may indicate retreat of the river mouth toward the coring site due to more frequent flooding or falling sea level, which suggests significant freshening of paleo-Daesan Bay and a decrease in the bay's size. This freshening period can be observed in other coastal bays. In early Stage 7, the TS% decreased markedly from 0.8% to 0.2% in Suncheon Bay (Fig. 6F), showing simultaneous changes. However, a slight decrease from 0.6% to 0.3% was observed in Goheung Bay (Fig. 6E), which suggests different sensitivities among locations.

Considering the relatively stable sea level during Stage 7, this difference appears to be caused by different responses to freshwater input or sea level changes between the two sites. In Goheung Bay today, freshwater input is easily diluted in the coastal area and its influence on salinity is weak. By contrast, in paleo-Daesan Bay, TS% and salinity appear to have been controlled by both past seawater inputs along the narrow channel connecting the bay to the open ocean and by direct precipitation inputs in the upper catchment of the Nakdong River. This description also can be applied to the Beolgyo tidal flat of Suncheon Bay, which is drained by the Belgyo stream. Notably, at present, salinity is highest during winter and decreases during summer due to freshwater influx into estuaries, which dilutes the salinity of seawater in coastal areas. Furthermore, during periods of high freshwater discharge from the main and small streams of the surrounding areas, mixing between surface and bottom water masses can be intensified, which may result in weakening of the anoxic conditions and blocking of seawater influx. These weakened anoxic conditions in the bottom water may have resulted in low TS%, probably due to reduced pyrite formation. Thus, the high-amplitude

salinity changes observed in the paleo-Daesan Bay can be attributed to the sensitivity (or vulnerability) of this area to freshwater inputs and sea level changes.

Stage 8 (ca. 3200–3100 cal yr BP): marine-brackish environment
Stage 8 appears to be the final period of seawater influence in paleo-Daesan Bay. TS% showed an abrupt increase from 0.2% to 0.7% (Fig. 6C). Similarly, C/S ratios decreased rapidly from 2 to 0.2, which suggests a strongly marine environment (Fig. 6B). During this stage, the estimated water depth appears to have been ~5–6 m, which still suggests a bay environment. However, the increase up to 40 in the C/N ratios indicates that sedimentary organic matter in the study site was mainly of terrestrial plants (Fig. 4), suggesting a final expansion of the coastal area and increased erosion responsible for the increase in terrestrial organic input. This salinity increase appeared synchronously with that in the Belgyo tidal flat at 3200 cal yr BP (Fig. 6). Thus, the observed peaks of high TS% may indicate intervals of sea level rise, resulting in both expansion of coastal areas and increased sandy sediment deposition with terrestrial plants.

Stage 9 (ca. 3100 cal yr BP–present): freshwater environment
Stage 9 began with an abrupt environmental change from high TS% to nearly zero TS% (Fig. 6B, C). This shift indicates a significant decrease in seawater influence along with decreased water depth to <4 m, and seawater inflow appears to have been blocked. This blocking and freshening may be related to several factors. The first factor to consider is the infilling of paleo-Daesan Bay. As shown in Figure 1, the paleo-water depth gradually decreased due to deposition of suspended materials transported by the Nakdong River, resulting in reduced accumulation space and seawater volume in the bay. This infilling process reduced the marine-affected area. As evidenced by the increased percentage of sand, the distance to the river mouth decreased. Finally, the bay evolved into a fluvial environment with channelization of the central part, accelerating river system development in the study area.

Long-term environmental changes in Daesan Basin and possible links to Holocene regional sea level changes

From the perspective of Holocene coastal evolution, marine transgression is an important feature of present coastal areas in East Asia, resulting in remarkable shifts from freshwater-dominant to marine-dominant environments due to Holocene sea level rise (Hori et al., 2004; Kim et al., 2012; Tanigawa et al., 2013; Cho et al., 2017; Katsuki et al., 2017; Xiong et al., 2020). Efforts to reconstruct regional sea level changes in East and South Asian coastal areas have been made. For example, regarding Early Holocene sea level changes on the Sunda Shelf in southeast Asia (Fig. 6), a representative far-field area, Bird et al. (2007) suggested that mean sea level rose rapidly from around −17 m at 9500 cal yr BP to around −3 m by 8000 cal yr BP. Xiong et al. (2020) suggested that sea level rose from −38.3 ± 1.6 m at 10,000 cal yr BP to its present height by 7000 cal yr BP in the inner part of the Hangzhou, east China. A similar increase was observed in the tectonically stable Toyooka Basin of western Japan. Relative sea level in the Toyooka Basin was estimated at −31.05 m in the Early Holocene (ca. 10,000 cal yr BP), above −4 m at 7900 cal yr BP, and −0.47 m in the middle Holocene (6700 cal yr BP), showing a gradual increasing trend (Tanigawa et al., 2013) (Fig. 6). During the Late Holocene, relative sea levels were near the present levels, with reports of +0.15 m at 3300 cal yr

BP and −0.37 m at 500 cal yr BP (Tanigawa et al., 2013). These changes likely caused environmental changes during the Holocene along the southern coast of Korea. However, changes in sea level along this coastal area have scarcely been studied. Therefore, we compared the long-term environmental evolution of "Paleo-Daesan Bay" and the Bibong-ri archeological site with available data on sea level changes, as described above, and investigated possible effects of sea level in the study area during the Holocene in terms of changes in salinity and water depth.

The Bibong-ri archeological site (Figs. 1, 6A), located on a tributary of Nakdong River, was clearly affected by Holocene transgression based on sea level indicators. This archeological site is famous for the occurrence of wooden boats, shell middens, and marine diatoms (Hwang et al., 2013). For example, shell layers (middens) composed mainly of oysters were found between −1.5 m and 0.8 m in elevation during the period of 7400–6100 cal yr BP (Fig. 6A), which corresponds to Stage 4, with the highest TS% in this study (Fig. 6B). Based on the presence of marine diatoms, Hwang et al. (2013) reported that these shell layers were within marine sediments. Interestingly, the elevations of the shell layers at 7400 and 7000 cal BP are very similar to the sea level of Toyooka Basin, Japan (Tanigawa et al., 2013), indicating a similar sea level in Bibong-ri and Toyooka at those times (Fig. 6A). This suggests that the shell layers formed around sea level at that time. The elevation of the shell layer at 6100 cal BP is similar to that of Chinese coastal areas (Lambeck et al., 2014, and references therein). The elevations of shell layers are 7–8 m higher than the depositional surface elevation in core STP18–06 from "paleo-Daesan Bay" at that time. This finding suggests that, during the period of 7400–6100 cal yr BP, seawater depth in the bay was at least 7–9 m. During the subsequent period between 6000–3000 cal yr BP, sea level appears to have decreased slightly, by only a few meters, based on reconstructed sea levels in Chinese coastal areas and Toyooka Basin in Japan, which suggests that paleo-seawater depth in the bay decreased from 8 m to 5 m during the Middle–Late Holocene (Stages 5∼8).

Consequently, in paleo-Daesan Bay, the TS% and salinity appear to have been controlled by both past seawater input along the narrow channel connecting this area to the open ocean and direct precipitation input from upper catchment areas of the Nakdong River. Among the observed fluctuations, low TS% and high C/S ratios clearly represent increased precipitation or falling sea level. By contrast, high TS% and low C/S ratios are linked to high or stable past sea levels. Furthermore, TS% shows a strong correlation with percentage of sand, which indicates that high salinity was linked to environments responsible for fine grain-size sediment deposition. In the bay environment, deposition of fine grain-sized materials indicates less-severe flooding, increased water depth, or an increase in coastal area. Thus, the peaks of high TS% might indicate intervals of rising sea level, resulting in both expansion of the coastal area and increase in fine-grain sediment deposition.

Duration of paleo-Daesan Bay and its implications for prehistoric human activities

Compared to regional sea level curves (Tanigawa et al., 2013; Lambeck et al., 2014, and references therein), the elevation of the STP18–05 site during Stage 1 appears to have been higher than relative sea level at that time, while Stage 2, with an abrupt increase in TS%, appears to have been below the sea level by 3–5 m (Fig. 6A, C). Although additional datasets are needed to determine the exact sea level in the study area during the Holocene, this comparison suggests that marine influence from seawater input (transgression) began ca. 8700 cal yr BP and that a dominantly marine-bay environment with water depth of ∼8 m had formed by ca. 8000 cal yr BP. Based on relative sea level curves from western Japan (Tanigawa et al., 2013) and Chinese coastal areas, as well as TS% measured in this study, water depth in paleo-Daesan Bay increased gradually with sea level rise and was ∼9 m at ca. 6000 cal yr BP, which suggests possible conditions of highstand and maximum coastal area. This gradual expansion of the coastal area in paleo-Daesan Bay during the period 8000–6000 cal yr BP could have provided stable conditions for development of marine cultures in the area with active seafaring, as indicated by the vessel relics of Bibong-ri site. Compared to the relatively stable marine environment of Goheung Bay (Fig. 6E), as demonstrated by low-amplitude changes in salinity (and TS%), paleo-Daesan Bay and inland coastal areas influenced by major river systems should be considered to have undergone significant salinity changes.

Fluctuations in the time series of TS% in paleo-Daesan Bay during the Middle–Late Holocene appear to be consistent with those recorded in Beolgyo tidal flat sediments from Suncheon Bay (Fig. 6F). Notably, the Beolgyo River drains into Suncheon Bay. Significant TS% decrease events on the Beolgyo tidal flat of Suncheon Bay (e.g., at 4100 cal yr BP) have been attributed to increases of freshwater input (or precipitation) based on geochemical and carbon isotope analyses (Lim et al., 2015). The common peaks in TS% at both paleo-Daesan Bay and Suncheon Bay (e.g., at 3200, 4700, 6100, 7600, 8500 cal yr BP; Fig. 6B, F) may indicate intervals of increased salinity, probably driven by decreases in freshwater input or sea level rise and the resulting expansion of coastal areas, leading to growth and prosperity of the marine culture.

By contrast, TS% fluctuations suggest that this area has been vulnerable to freshening, which may have caused cultural disruption at multi-centennial to millennial timescales. Furthermore, the present study provides a good example of the interruption of marine cultures in inland areas during the Late Holocene. A remarkable shift is demonstrated by the abrupt decrease in TS% to zero at 3100 cal yr BP and the continuously freshwater environment since then. Marine cultures, for example at the Bibong-ri site, could have flourished during the period of ca. 8000–3200 cal yr BP in the area surrounding paleo-Daesan Bay. It is important to note that past studies in this area (e.g., Kaneko, 2008; Kwak et al., 2020; Kim et al., 2021) have focused on the human activity and their relics over hundreds of years, revealing diverse seasonal marine and terrestrial resources during the Middle Holocene (Kaneko, 2008; Kwak et al., 2020; Kim et al., 2021). These prehistorical studies should incorporate information regarding inland coastal evolution (e.g., paleo-Daesan Bay) during the Middle–Late Holocene.

Paleo-sulfur information and its implications for East Asian prehistoric human activities

In eastern China, efforts have been made to reconstruct past sea level changes and their influences on prehistorical cultures (Zong et al., 2011; Sun et al., 2019; Huang et al., 2020, 2021). Interestingly, the ages of shell middens at the Bibong-ri prehistoric site and of shell fragments in this study are quite similar to the emergence ages (7000–6000 cal yr BP) of archaeological sites in the northern highlands of the Jiangsu region along the east coast of China, as well as human inhabitation at ca. 6500

cal yr BP on the Taihu Plain (Li et al., 2018), which suggests possible similarity in the responses to past sea level changes. Recently, Huang et al. (2021) explored the possible responses of Neolithic people to past extreme typhoon events at the Xiawangdu site on Ningbo Plain, on the east coast of China, during the Middle–Late Holocene. They suggested that Neolithic people may have abandoned low-lying land near the river channel or retreated to dwellings constructed on earthen mounds during the flooding (Huang et al., 2021).

To investigate the simultaneous responses of Neolithic people in coastal areas of Korea and China during the Holocene events in further detail, comparison of common environmental indicators related to the direct influence of seawater is necessary. This study suggests that sulfur data (e.g., TS% or C/S ratios) is helpful for tracing seawater movement, providing background information for such studies on the east coast of China. Previous studies indicate that water depth was sufficient for the evolution of estuary and bay environments in eastern coastal areas, influencing settlement patterns of prehistoric humans. TS% and C/S ratios, relatively conventional and simple indices, will be useful for reconstructing spatial and temporal sea water influences in East Asia. This information can characterize changes to support tracing of possible sea level fluctuations over centennial to millennial timelines at regional scales and assessment of the mechanisms controlling such high-resolution sea level instability.

CONCLUSIONS

We investigated the physical and geochemical features of 20-m-long sedimentary cores from the previously seawater-filled Daesan Basin located along the middle reach of the present Nakdong River in Korea. Based on the relationships among lithological (e.g., sand%) and geochemical (TOC levels, TS%, and their ratio [C/S ratio]) characteristics, Holocene riverine and coastal environments can be divided into three periods and nine stages: a weak freshwater period (before 8500 cal yr BP), brackish-marine period (8500–3000 cal yr BP), and strong freshwater period (since 3000 cal yr BP). The first transgression event was detected at ca. 8500 cal yr BP due to seawater influx along the present Nakdong River. After subsequent weakening of the seawater influence due to the 8.2 ka cold event, higher TS% (0.8–1%) and interbedded fossil oysters during 8000–6000 cal yr BP indicate highstand at 6100 cal yr BP and dominantly marine environments, forming paleo-Daesan Bay with water depth of ~10–8 m.

Interestingly, marked fluctuations in geochemical indicators occurred during the Early–Late Holocene, with increased TS% and decreased C/S ratios at 3700, 4200, 6500, 7600, and 8500 cal yr BP, suggesting intensified seawater influences and resultant high salinities in the study area at those times. These periods of intensified salinity are similar to those observed in coastal sedimentary records from Suncheon Bay and Goheung Bay along the southern coast of Korea, which indicates regional-scale responses to sea level or hydroclimatic changes. The dominant marine environment (paleo-Daesan Bay) from ca. 8000–3100 cal yr BP in a remote inland area provides a useful analog for inland paleo-bay studies in East Asia and the interpretation of prehistoric human activities and their remains, such as boats and shell middens, in terms of sea level changes.

REFERENCES

Abbott, M.B., Stafford, T.W., Jr., 1996. Radiocarbon geochemistry of modern and ancient Arctic lake systems, Baffin Island, Canada. *Quaternary Research* **45**, 300–311.

Alley, R.B., Mayewski, P.A., Sowers, T., Stuiver, M., Taylor, K.C., Clark, P.U., 1997. Holocene climatic instability: a prominent, widespread event 8200 yr ago. *Geology* **25**, 483–486.

Berner, R.A., 1984. Sedimentary pyrite formation: an update. *Geochimica et Cosmochimica Acta* **48**, 605–615.

Berner, R.A., Raiswell, R., 1984. C/S method for distinguishing freshwater from marine sedimentary rocks. *Geology* **12**, 365–368.

Bird, M.I., Fifield, L.K., Teh, T.S., Chang, C.H., Shirlaw, N., Lambeck, K., 2007. An inflection in the rate of early mid-Holocene eustatic sea-level rise: a new sea-level curve from Singapore. *Estuarine, Coastal and Shelf Science* **71**, 523–536.

Blaauw, M., 2010. Methods and code for 'classical' age-modelling of radiocarbon sequences. *Quaternary Geochronology* **5**, 512–518.

Bronk Ramsey, C., 2009a. Bayesian analysis of radiocarbon dates. *Radiocarbon* **51**, 337–360.

Bronk Ramsey, C., 2009b. Dealing with outliers and offsets in radiocarbon dating. *Radiocarbon* **51**, 1023–1045.

Cho, A., Cheong, D., Kim, J.C., Shin, S., Park, Y.H., Katsuki, K., 2017. Delta formation in the Nakdong River, Korea, during the Holocene as inferred from the diatom assemblage. *Journal of Coastal Research* **33**, 67–77.

Dykoski, C.A., Edwards, R.L., Cheng, H., Yuan, D., Cai, Y., Zhang, M., Lin, Y., Qing, J., An, Z., Revenaugh, J., 2005. A high-resolution, absolute-dated Holocene and deglacial Asian monsoon record from Dongge Cave, China. *Earth and Planetary Science Letters* **233**, 71–86.

Hasegawa, T., Hibino, T., Hori, S., 2010. Indicator of paleosalinity: sedimentary sulfur and organic carbon in the Jurassic–Cretaceous Tetori Group, central Japan. *Island Arc* **19**, 590–604.

Hong, W, Park J.H., Kim K.J., Woo, H.J., Kim, J.K., Choi, H.K., Kim, G.D., 2010a. Establishment of chemical preparation methods and development of an automated reduction system for AMS sample preparation at KIGAM. *Radiocarbon* **52**, 1277–1287.

Hong, W, Park, J.H., Sung, K.S., Woo, H.J., Kim, J.K., Choi, H.W., Kim, G.D., 2010b. A new1MV AMS facility at KIGAM. *Radiocarbon* **52**, 243–251.

Hori, K., Tanabe, S., Saito, Y., Karuyama, S., Nguyen, V., Kitamura, A., 2004. Delta initiation and Holocene sea-level change: example from the Song Hong (Red River) Delta, Vietnam. *Sedimentary Geology* **164**, 237–249.

Huang, J., Lei, S., Tang, L., Wang, A., Wang, Z., 2020. Mid-Holocene environmental change and human response at the Neolithic Wuguishan site in the Ningbo coastal lowland of East China. *The Holocene* **30**, 1591–1605.

Huang, J., Li, Y., Ding, F., Zheng, T., Meadows, M.E., Wang, Z., 2021. Sedimentary records of mid-Holocene coastal flooding at a Neolithic site on the southeast plain of Hangzhou Bay, east China. *Marine Geology* **431**, 106380. https://doi.org/10.1016/j.margeo.2020.106380.

Hu, C., Henderson, G.M., Huang, J., Xie, S., Sun, Y., Johnson, K.R., 2008. Quantification of Holocene Asian monsoon rainfall from spatially separated cave records. *Earth and Planetary Science Letters* **266**, 221–232.

Hwang, S., Kim, J.Y., Yoon, S.O., 2013. Sea level change during the Middle Holocene at Bibong-ri, Changnyeong-gun, Gyeongsangnam-do, South Korea. *Journal of the Korean Geographical Society* **48**, 837–855. [In Korean with English abstract]

Innes, J.B., Zong, Y., Xiong, H., Wang, Z., Chen, Z., 2019. Pollen and non-pollen palynomorph analyses of Upper Holocene sediments from Dianshan, Yangtze coastal lowlands, China: hydrology, vegetation history and human activity. *Palaeogeography, Palaeoclimatology, Palaeoecology* **523**, 30–47.

Ishihara, T., Sugai, T., Hachinohe, S., 2012. Fluvial response to sea-level changes since the latest Pleistocene in the near-coastal lowland, central Kanto Plain, Japan. *Geomorphology* **147–148**, 49–60.

Jaraula, C.M.B., Siringan, F.P., Klingel, R., Sato, H., Yokoyama, Y., 2014. Records and causes of Holocene salinity shifts in Laguna de Bay, Philippines. *Quaternary International* **349**, 207–220.

Kaneko H., 2008. Animal remains from Changnyeong Bibong-ri Site. In: Gimhae National Museum (Ed.), *Bibong-ri Site, Changnyeong: The Neolithic Low-Lying Wetland Site. Report on the Research of Antiquities of the Gimhae National Museum.* Vol. 6. Gimhae: Gimhae National Museum Press. p. 305–390. [in Korean and Japanese]

Kato, M., Fukusawa, H., Yasuda, Y., 2003. Varved lacustrine sediments of Lake Tougou-ike, western Japan, with reference to Holocene sea-level changes in Japan. *Quaternary International* **105**, 33–37.

Katsuki, K., Nakanishi, T., Lim, J., Nahm, W.H., 2017. Holocene salinity fluctuations of the East Korean lagoon related to sea level and precipitation changes. *Island Arc* **26**, e12214. https://doi.org/10.1111/iar.12214.

Kendall, R.A., Mitrovica, J.X., Milne, G.A., Törnqvist, T.E., Li, Y., 2008. The sea-level fingerprint of the 8.2 ka climate event. *Geology* **36**, 423–426.

Kigoshi, K., Suzuki, N., Shiraki, M., 1980. Soil dating by fractional extraction of humic acid. *Radiocarbon* **22**, 853–857.

Kim, H., Lee, H., Lee, G.A., 2021. New marine reservoir correction values (ΔR) applicable to dates on Neolithic shells from the south coast of Korea. *Radiocarbon* **63**, 1287–1302.

Kim, J.C., Cheong, D., Shin, S., Park, Y.H., Hong, S.S., 2015. OSL chronology and accumulation rate of the Nakdong deltaic sediments, southeastern Korean Peninsula. *Quaternary Geochronology* **30**, 245–250.

Kim, J.C., Eum, C.H., Yi, Kim, J.Y., Hong, S.S., Lee, J.Y., 2012. Optically stimulated luminescence dating of coastal sediments from southwestern Korea. *Quaternary Geochronology* **10**, 218–223.

Koma, T., Suzuki, Y., 1988. Total sulfur content of late Quaternary sediments in Shibakawa lowland, Saitama Prefecture, central Japan, and its relation to the sedimentary environment. *Chemical Geology* **68**, 221–228.

Kretschmer, W., Anton, G., Bergmann, M., Finckh, E., Kowalzik, B., Klein, M., Leigart, M., et al., 1997. ^{14}C dating of sediment samples. *Nuclear Instruments and Methods in Physics Research B* **123**, 455–459.

Kwak, S.K., Obata, H., Lee, G.-A., 2020. Broad-spectrum foodways in southern coastal Korea in the Holocene: isotopic and archaeobotanical signatures in Neolithic shell middens. *The Journal of Island and Coastal Archaeology* **17**, 97–125.

Lamb, A., Wilson, G.P., Leng, M.J., 2006. A review of coastal palaeoclimate and relative sea-level reconstructions using δ^{13}C and C/N ratios in organic material. *Earth-Science Reviews* **75**, 29–57.

Lambeck, K., Rouby, H., Purcell, A., Sun, Y., Sambridge, M., 2014. Sea level and global ice volumes from the Last Glacial Maximum to the Holocene. *Proceedings of the National Academy of Sciences* **111**, 15296–15303.

Li, L., Zhu, C., Qin, Z., Storozum, M.J., Kidder, T.R., 2018. Relative sea level rise, site distributions, and Neolithic settlement in the Early to Middle Holocene, Jiangsu Province, China. *The Holocene* **28**, 354–362.

Lim, J., Lee, J.Y., Hong, S.S., Park, S., Lee, E., Yi, S., 2019. Holocene coastal environmental change and ENSO-driven hydroclimatic variability in East Asia. *Quaternary Science Reviews* **220**, 75–86.

Lim, J., Lee, J.Y., Kim, J.C., Hong, S.S., Yang, D.Y., 2015. Holocene environmental change at the southern coast of Korea based on organic carbon isotope (δ^{13}C) and C/S ratios. *Quaternary International* **384**, 160–168.

Meyers, P.A., 1997. Organic geochemical proxies of palaeoceanographic, palaeolimnologic, and palaeoclimatic processes. *Organic Geochemistry* **27**, 213–250.

Nahm, W.-H., Kim, J.C., Bong, P.-Y., Kim, J.-Y., Yang, D.-Y., Yu, K.-M., 2008. Late Quaternary stratigraphy of the Yeongsan Estuary, Southwestern Korea. *Quaternary International* **176–177**, 13–24.

Nakai, N., Ohta, T., Fujisawa, H., Yoshida, M., 1982. Paleoclimatic and sea-level changes deduced from organic carbon isotope ratios, C/N ratios and

pyrite contents of cored sediments from Nagoya Harbor, Japan. *The Quaternary Research (Daiyonki-Kenkyu)* **21**, 169–177. [in Japanese]

Nakanishi, T., Hong, W., Sung, K.S., Lim, J., 2013. Radiocarbon reservoir effect from shell and plant pairs in Holocene sediments around the Yeongsan River in Korea. *Nuclear Instruments and Methods in Physics Research Section B: Beam Interactions with Materials and Atoms* **294**, 444–451.

Nakanishi, T., Hong, W., Sung, K.S., Sung, K.H., Nakashima, R., 2015. Offsets in radiocarbon ages between plants and shells from same horizons of coastal sediments in Korea. *Nuclear Instruments and Methods in Physics Research Section B: Beam Interactions with Materials and Atoms* **361**, 670–679.

Nguyen, V.L., Tateishi, M., Kobayashi, I., 1998. Reconstruction of sedimentary environments for Late Pleistocene to Holocene coastal deposits of Lake Kamo, Sado Island, Central Japan. *The Quaternary Research* **37**, 77–94.

Park, J., Park, J., Yi, S., Kim, J.C., Lee, E., Jin, Q., 2018. The 8.2 ka cooling event in coastal East Asia: high-resolution pollen evidence from southwestern Korea. *Scientific Reports* **8**, 12423. https://doi.org/10.1038/s41598-018-31002-7.

Reimer, P.J., Bard, E., Bayliss, A., Beck, J.W., Blackwell, P.G., Bronk Ramsey, C., Buck, C., et al., 2013. IntCal13 and Marine13 radiocarbon age calibration curves 0–50,000 years cal BP. *Radiocarbon* **55**, 1869–1887.

Sampei, Y., Matsumoto, E., Kamei, T., Tokuoka, T., 1997. Sulfur and organic carbon relationship in sediments from coastal brackish lakes in the Shimane peninsula district, southwest Japan. *Geochemical Journal* **31**, 245–262.

Stanley, D.J., Warne, A.G., 1994. Worldwide initiation of Holocene marine deltas by deceleration of sea level rise. *Science* **265**, 228–231.

Sun, Q., Liu, Y., Wünnemann, B., Peng, Y., Jiang, X., Deng, L., Chen, J., Li, M., Chen, Z., 2019. Climate as a factor for Neolithic cultural collapses approximately 4000 years BP in China. *Earth-Science Reviews* **197**, 102915. https://doi.org/10.1016/j.earscirev.2019.102915.

Takata, H., Khim, B.K., Shin, S., Lee, J.Y., Kim, J.C., Katsuki, K., Cheong, D., 2019. Early to Middle Holocene development of the Tsushima Warm Current based on benthic and planktonic foraminifera in the Nakdong River delta (southeast Korea). *Quaternary International* **519**, 183–191.

Tanigawa, K., Hyodo, M., Sato, H., 2013. Holocene relative sea-level change and rate of sea-level rise from coastal deposits in the Toyooka Basin, western Japan. *The Holocene* **23**, 1039–1051.

Tan, L., Li, Y., Wang, X., Cai, Y., Lin, F., Cheng, H., Edwards, R.L., 2020. Holocene monsoon change and abrupt events on the western Chinese Loess Plateau as revealed by accurately dated stalagmites. *Geophysical Research Letters* **47**, e2020GL090273. https://doi.org/10.1029/2020GL09027.

Törnqvist, T.E., Bick, S.J., González, J.L., van der Borg, K., de Jong, A.F., 2004. Tracking the sea-level signature of the 8.2 ka cooling event: new constraints from the Mississippi Delta. *Geophysical Research Letters* **31**, L23309. https://doi.org/10.1029/2004GL021429.

Woolfe, K.J., Dale, P.J., Brunskill, G.J., 1995. Sedimentary C/S relationships in a large tropical estuary: evidence for refractory carbon inputs from mangroves. *Geo-Marine Letters* **15**, 140–144.

Xiong, H., Zong, Y., Li, T., Long, T., Huang, G., Fu, S., 2020. Coastal GIA processes revealed by the Early to Middle Holocene sea-level history of east China. *Quaternary Science Reviews* **233**, 106249. https://doi.org/10.1016/j.quascirev.2020.106249.

Yang, D.Y., Kim, J.-Y., Nahm, W.-H., Ryu, E., Yi, S., Kim, J.C., Lee, J.-Y., Kim, J.-K., 2008. Holocene wetland environmental change based on major element concentrations and organic contents from the Cheollipo coast, Korea. *Quaternary International* **176–177**, 143–155.

Yoo, D.G., Kim, S.P., Chang, T.S., Kong, G.S., Kang, N.K., Kwon, Y.K., Park, S.C., 2014. Late Quaternary inner shelf deposits in response to Late Pleistocene–Holocene sea level changes: Nakdong River, SE Korea. *Quaternary International* **344**, 156–169.

Zong, Y., Innes, J.B., Wang, Z., Chen, Z., 2011. Mid-Holocene coastal hydrology and salinity changes in the east Taihu area of the lower Yangtze wetlands, China. *Quaternary Research* **76**, 69–82.